



Activation of 20-HETE Synthase Triggers Oxidative Injury and Peripheral Nerve Damage in Type 2 Diabetic Mice

Mary Haddad,^{*,†} Stéphanie Eid,^{*} Frederic Harb,[‡] Mohamed E.L. Massry,^{*} Sami Azar,^{§,¶} Erik-Andre Sauleau,[†] and Assaad A. Eid^{*,¶}

^{*}Department of Anatomy, Cell Biology and Physiological Sciences, Faculty of Medicine and Medical Center, American University of Beirut, Beirut, Lebanon, [†]Department of Biostatistics, Centre National de la Recherche Scientifique (CNRS) Unité Mixte de Recherche (UMR) 7357 ICube, University of Strasbourg, Strasbourg, France, [‡]Department of Life and Earth Sciences, Faculty of Sciences, Lebanese University, Fanar, Lebanon, [§]Department of Internal Medicine, Division of Diabetes and Endocrinology, Faculty of Medicine and Medical Center, American University of Beirut, Beirut, Lebanon, [¶]AUB Diabetes, American University of Beirut, Beirut, Lebanon

Abstract: Diabetic Peripheral Neuropathy (DPN), highly prevalent among patients with diabetes, is characterized by peripheral nerve dysfunction. Reactive Oxygen Species (ROS) overproduction has been suggested to orchestrate diabetic complications including DPN. Untargeted antioxidant therapy has exhibited limited efficacy, highlighting a critical need to explore ROS sources altered in a cell-specific manner in DPN. Cytochromes P450 (CYP) enzymes are prominent sources of ROS. Particularly, the 20-HETE synthase, CYP4A, is reported to mediate diabetes-induced renal, retinal, and cardiovascular injuries. This work investigates the role of CYP4A/20-HETE in DPN and their mechanisms of action. Non-obese type 2 Diabetic mice (MKR) were used and treated with a CYP4A-inhibitor (HET0016) or AMPK-activator (Metformin). Peripheral nerves of MKR mice reflect increased CYP4A and 20-HETE levels, concurrent with altered myelin proteins and sensorimotor deficits. This was associated with increased ROS production and altered Beclin-1 and LC3 protein levels, indicative of disrupted autophagic responses in tandem with AMPK inactivation. AMPK activation via Metformin restored nerve integrity, reduced ROS production, and regulated autophagy. Interestingly, similar outcomes were revealed upon HET0016 treatment whereby ROS production, autophagic responses, and AMPK signaling were normalized in diabetic mice. Altogether, the results highlight hyperglycemia-mediated oxidative injury in DPN through a novel CYP4A/20-HETE/AMPK pathological axis.

Perspective: To our knowledge, this is the first study to highlight the role of CYPs/20-HETE-induced oxidative injury in the pathogenesis of diabetic peripheral neuropathy. Targeting the identified pathological axis CYP4A/20-HETE/AMPK may be of clinical potential in predicting and alleviating peripheral nerve injury in patients with Type 2 Diabetes Mellitus.

© 2022 The Author(s). Published by Elsevier Inc. on behalf of United States Association for the Study of Pain, Inc. This is an open access article under the CC BY-NC-ND license

(<http://creativecommons.org/licenses/by-nc-nd/4.0/>)

Key words: Diabetic peripheral neuropathy, insulin resistance, 20-HETE, AMPK, oxidative stress.

Received July 7, 2021; Revised January 26, 2022; Accepted February 24, 2022.

This work was funded by a Medical Practice Plan Grant from the American University of Beirut to AAE.

All Authors reports no conflict of interest.

Address reprint requests to Assaad A. Eid, Department of Anatomy, Cell Biology and Physiological Sciences, Faculty of Medicine and Medical Center, American University of Beirut, Bliss Street, 11-0236, Riad El-Solh

1107-2020, Lebanon. E-mail: ae49@aub.edu.lb
1526-5900/\$36.00

© 2022 The Author(s). Published by Elsevier Inc. on behalf of United States Association for the Study of Pain, Inc. This is an open access article under the CC BY-NC-ND license

(<http://creativecommons.org/licenses/by-nc-nd/4.0/>)

<https://doi.org/10.1016/j.jpain.2022.02.011>

D iabetic Peripheral Neuropathy (DPN) is the prevalent type of neuropathy in diabetes. DPN is a disorder of sensory nerves early in the course of the disease whereby fibers undergo degeneration, axonal atrophy, and demyelination with limited regenerative potential.^{16,41} Clinically, DPN manifests as abnormal sensations, motor dysfunctionality, and disabling pain at later stages.⁶⁰ Despite optimal management of diabetes, the risk of DPN progression remains high with a poorly understood pathobiology.

Reactive Oxygen Species (ROS) overproduction poses a pathogenic state in multiple organs.^{11,36} The specific inhibition of certain sources ameliorates diabetic renal, retinal, neural, and cardiac complications.^{1,12,13,15,51} In DPN, oxidative stress mediates injury to the vasa nervorum and/or vascular endothelia and neurons^{28–48} but limited studies investigate the effect on Schwann cell (SC) physiology and myelination. Our group shows the attenuation of diabetes-induced activation of NADPH-oxidases and ROS production to confer anti-apoptotic effects, and neuroprotection to SCs and peripheral nerves.¹⁵ Yet, further investigation warrants identifying other sources of ROS involved in DPN.

While antioxidant therapies target inflammation, biochemical perturbances, or organelle-dependent ROS production in DPN, their integration into clinical practice was unsuccessful,^{26,29,40,48,57} urging targeted approaches for the management of DPN.

Cytochromes P450 enzymes are potent sources of ROS, produced as a byproduct of reactions they catalyze.^{14,58} The CYP4A ω -hydroxylase converts arachidonic acid to 20-hydroxyeicosatetraenoic acid (20-HETE), a bioactive metabolite whose effect is site and cell specific.^{51,58} 20-HETE synthase has been shown to have high physiological relevance in maintaining homeostasis, vascular tone, and blood flow.^{1,51} However, recent studies report 20-HETE alterations to mediate obesity, hyperglycemia, deficient insulin responses,^{19,32} oxidative stress⁵⁸ and the onset of diabetic renal, retinal, and cardiac complications.^{1,13,51} Yet, the role of 20-HETE in the nervous system (NS) is understudied. In the central NS, CYP4A is highly expressed in cells lining the neurovascular unit, with 20-HETE playing developmental and regulatory roles, inflammation, and oxidative injury in neurodegenerative diseases.^{21,47} To date, no studies have investigated CYP4A/20-HETE in the peripheral NS (PNS) nor DPN.

Myelin Protein Zero (MPZ) and Peripheral Myelin Protein 22 (PMP22) are produced by SCs and determine the precise arrangement and function of the myelin sheath.²⁴ They are also markers of neuronal injury, myelin integrity and functionality whereby alterations in either protein insults SCs, neuronal function, and signal exchange in the PNS.^{15,18,23} Moreover, defected PMP22 forms cytotoxic aggregates^{18,23} that are cleared by the cellular autophagic response responsible for resource homeostasis. However, these responses are defective in demyelinating neuropathies.^{20,43} Additionally, AMP-activated protein kinase (AMPK) is a key signaling pathway that governs cellular activities in response to metabolic cues. Emerging studies show

that impaired AMPK activity mediates metabolic stress, diabetes-related injuries.^{12,39,45} and insulin resistance.⁵⁵ In the NS, AMPK moderates neuronal functions, and survival, with a dual role in modulating autophagy in conditions such as chronic pain and diabetes.^{2,6,35,45,49}

In this study, MKR transgenic murine model for type 2 diabetes (T2DM), characterized by MKR promoter knockdown in skeletal muscles which triggers peripheral insulin resistance without the development of obesity were used. These features are robust for the study of diabetic complications from the standpoint of hyperglycemia and insulin-resistance.¹⁷ This work explores mechanisms of DPN pathogenesis and identifies 20-HETE synthase, CYP4A, as a source of ROS triggering oxidative peripheral nerve injury through autophagy deregulation, AMPK inactivation and myelin protein disruption as hallmarks of cellular injury. Altogether, understanding this pathological axis and its involvement in DPN may introduce adjunct therapies.

Methods

Animal Studies

All animal work was conducted according to the National Institute of Health guidelines and approved by the Institutional Animal Care and Use Committee at the American University of Beirut. MKR (FVB-Tg (Ckm-IGF1R*K1003R)1Dlr/J) male mice (Jackson laboratories, Bar Harbor, Maine, USA) weighing 25 grams on average were used. These mice exhibit the genotypic and phenotypic profiles of human type 2 diabetes (T2DM) and develop hyperglycemia starting 8 weeks of age¹⁷. Age-matched FVB/NJ males served as the normoglycemic, control group. The animals were randomly grouped into 3 subsets 1) non-diabetic controls treated with the corresponding vehicle (FVB-Ctr) 2) untreated diabetics (MKR-Db) treated with the corresponding vehicle 3) diabetics treated with HET0016 (MKR-Db + HET0016) or Metformin (MKR-Db + Metformin). A total of 3 to 4 mice were placed per cage and strict measures were taken to alleviate suffering and pain. The group size required to detect a 25% increase in the expression of the protein of interest or functional changes with a significance (α) of 5% and a power (β) of 80% (assuming a standard deviation of 25% for control) will be 11 for each group. HET0016 (Cayman Chemicals, MI, USA) is a specific 20-HETE synthase and/or CYP4A inhibitor which was administered subcutaneously and daily for a period of 10 weeks at a dose of 2.5 mg/kg¹³. Metformin, an activator of the AMPK signaling pathway, was administered daily by intraperitoneal injection at a dose of 150 mg/kg for 13 weeks.³⁹ HET0016 and metformin were prepared as previously described.^{1,31} Both drugs were administered at the same time of the day after 10 weeks of diabetes onset. All animals were kept in standard cages in a temperature-controlled room (25°C), on a 12 of 12-dark and/or light cycle and had ad libitum access to standard chow and water. Random blood glucose levels were monitored via tail vein

punctures. At sacrifice, blood was collected after isoflurane inhalation by the animals followed by cervical dislocation and sciatic nerves collection. Glycosylated hemoglobin (HbA1c) levels were assessed via an ELIZA kit according to manufacturer's protocol (Crystal Chem Inc).

Functional Assessment for Neuropathy

Peripheral nerve function was further assessed via electrophysiological assessment of the Nerve Conduction Velocity (NCV) as previously described.¹⁵ NCV measures were performed in anaesthetized mice at 32–34°C using a heating pad. Motor Nerve Conduction Velocity (MNCV) was determined by measuring compound muscle action potentials using supramaximal stimulation distally at the ankle and proximally at the sciatic notch. Sensory Nerve Conduction Velocity (SNCV) was recorded behind the median malleolus in the digital nerve to the second toe by stimulating with the smallest current that resulted in a maximal amplitude response. The NCV was calculated by dividing the distance between the cathode positions by the difference in distal from proximal latencies.

Behavioral Assessment for Neuropathy

To assess motor coordination and balance, the Raised Beam Walking test was performed as previously described.³⁴ Briefly, animals were placed on a platform above a flat surface. Animals were placed for habituation and then trained to cross the platform. Once able to perform the test, the time taken to cross the platform, the speed, the number of stops and the number of faults and/or slips were recorded for analysis over 3 separate trials. To assess thermal analgesia and pain perception, the Hind Paw Withdrawal test was performed.⁹ The IITC plantar Analgesia meter was used. The test features a heating beam set at an idle intensity of 2% and active intensity of 25% with a cut-off time set at 20 seconds and a platform set at 32 °C for acclimation. The thermal stimulus was targeted at the hind paw of animals and the time to sense the heat and withdraw their paws was recorded for analysis, 6 measurements per mouse. The final test assessed muscle tone and neuromuscular strength via the Grip Strength test.⁴ Animals were trained to hang using their forelimbs from a stand until their grip fails. The time spent hanging was recorded over 3 consecutive days.

ROS Detection by Confocal Microscopy

Dihydroethidium (DHE) is an oxidative, cell-permeable fluorescent dye that undergoes a 2 electron oxidation upon interaction with superoxide anions, H₂O₂ or cellular processes involving peroxidases, oxidases, or cytochrome C to form the DNA-binding fluorophore ethidium bromide. To detect intracellular reactive oxygen species (ROS) throughout the axoplasm in nerve fiber bundles, DHE staining was carried out as previously described.³⁶ Briefly, unfixed, frozen sciatic nerves were

embedded in Optimal Cutting Temperature compound and then cut into 4 μm thick cross-sections and placed on glass slides. DHE (20 μmol/l) was applied to each tissue section, and the slides were incubated in a light-protected humidified chamber at 37°C for 30 min. Upon DHE interaction with intracellular ROS, ROS production from cytosol or nuclei was demonstrated by red fluorescent labeling. Fluorescence images of ethidium-stained tissue were obtained with a laser-scanning confocal microscope (Zeiss, LSM 710). Fluorescence was detected at 561 nm long-pass filter. ROS production was demonstrated. The average of 4 areas per section stained with DHE was taken as the value for each animal. Zen light Software was used for the quantification of the intensity of DHE stain.

ROS Detection by High Performance Liquid Chromatography

Superoxide-specific production was further assessed via High Performance Liquid Chromatography as previously described.^{1,15} Sciatic nerve homogenates were washed with Hanks balanced salt solution (HBSS)-diethylenetriaminepentaacetic acid (DTPA) twice and incubated for 30 min with 50 μM DHE (Sigma-Aldrich) in HBSS–100 μM DTPA. Tissues were then processed for analysis. Tissues were harvested in acetonitrile and centrifuged (12,000 X g for 10 min at 4°C). The homogenate was dried under vacuum and analyzed by HPLC with fluorescence detectors. Quantification of DHE, EOH, and ethidium concentrations was performed by comparison of integrated peak areas between the obtained and standard curves of each product under chromatographic conditions identical to those described above. EOH and ethidium fluorescence was detected with excitation at 510 nm and emission at 595 nm, whereas DHE fluorescence was detected by UV absorption at 370 nm. The results are expressed as the amount of EOH produced (nmol) normalized for the amount of DHE consumed (μmol).

20-HETE Production by High Performance Liquid Chromatography

Levels of 20-HETE were measured in sciatic nerves by HPLC. In short, [1-14C]-labeled arachidonic acid (50–100 μmol/l) was dried down and resuspended in the reaction mix containing 50 μg microsomes, 30 mmol/l isocitrate, and 0.2-unit isocitrate dehydrogenase in reaction buffer (100 mmol/l potassium phosphate, pH 7.4, 5 mmol/l magnesium chloride, and 1 mmol/l EDTA). After incubation at 37°C for 5 min, the reaction was initiated by the addition of NADPH to a final concentration of 1 mmol/l. Aliquots were removed at 30, 60, and 90 min, and the reaction was stopped by the addition of 100% methanol. The precipitated proteins were then pelleted by centrifugation (in a microcentrifuge), and the samples were stored at -20°C until analyzed. The metabolites were separated via HPLC on a C-18 column using an acetonitrile and/or H₂O gradient and identified by coelution with labeled standards.¹³

NADPH Oxidase Activity Assay

Proteins were extracted from crushed frozen sciatic nerves in a lysis buffer (20 mM KH₂PO₄ (pH 7.0), 1 mM EGTA, 1 mM phenylmethylsulphonyl fluoride, 10 μ g/ml aprotinin, and 0.5 μ g/ml leupeptin). After tissue lysis with lysis buffer, homogenates protein content was then quantified using the Lowry Protein Assay. The assay reaction contained 25 μ g of homogenates added to 50 mM phosphate buffer (pH 7.0), 1 mM EGTA, 150 mM sucrose, 5 μ M lucigenin, and 100 μ M NADPH. Photon emission expressed as relative light units (RLU) was measured every 30s for 5 minutes in a luminometer. Superoxide production was expressed as relative light units/min/mg of protein.^{11,13}

Immunohistochemistry

Paraffin embedded, formalin-fixed sciatic nerves were cut into 5 μ m sections and fixed onto star-frosted slides. Sections were deparaffinized by incubation at 56°C for 50 minutes. Then they were immersed in xylene, rehydrated in a descending alcohol gradient, and distilled water. Sections were then incubated with sodium citrate buffer in a humidified chamber for 1 hour for antigen retrieval. The subsequent reactions were performed using Novolink Polymer Detection Kit (RE7150-K) (Leica Biosystems, Wetzlar, Germany) according to manufacturer instructions and at room temperature. Sections were stained overnight at 4°C with Beclin-1 (1:100) and LC3B protein (1:100) (Cell Signaling, Massachusetts, USA), processed on the following day for visualization after signal development with post-primary Rabbit anti mouse IgG (<10 μ g/mL) in 10% (v/v) animal serum in tris-buffered saline/0.1% ProClin™ 950. Slides were then incubated with Novolink polymer Anti-rabbit Poly-HRP-IgG, and DAB chromogen according to kit protocol. Slides were then counterstained using hematoxylin, dehydrated, and mounted. Slides were examined using the Olympus CX41 microscope by a blinded observer. A positive signal is reflected by the detection of colored brown pixels corresponding to fluorescently tagged primary antibodies, against the hematoxylin counterstain. Slides were quantified using the color deconvolution plugin with NIH ImageJ software.

Western Blotting

Mouse sciatic nerves were lysed using RIPA buffer and prepared as previously described.^{11,13} For immunoblotting, 20-40 μ g of proteins were separated on 12 to 15% polyacrylamide gel Electrophoresis and transferred to nitrocellulose membranes (Bio-Rad, California, USA). The blots were blocked with 5% BSA in Tris-buffered saline and then incubated overnight with anti-CYP4A (1:2000, Abcam, Cambridge, United Kingdom), anti-P0 and anti-PMP22 (1:1000, Sigma Aldrich, Missouri, USA), Beclin-1 (1:1000), LC3B (1:500), and pAMPK^{Thr172} (1:1000) (Cell Signaling, Massachusetts, USA). HSC (1:1000) and GAPDH (1:1000) (Santa Cruz Biotechnology Inc. Texas, USA) were used as housekeeping, loading controls. The primary antibodies were detected using

horseradish peroxidase-conjugated IgG (1:3000, Bio-Rad, California, USA). Bands were visualized by enhanced chemiluminescence. Densitometric analysis was performed using Image J software. We emphasize that the quantifications of the described data are normalized accordingly depending on the loading control reported in each representative figure.

PMP22 Aggregation Assay

PMP22 is 1 of the aggregate-prone proteins that forms aggresomes when mutated or proteasomal activity is impaired. Accumulation of PMP22 aggregates has been linked to neurodegeneration and neuropathies. PMP22 aggregation is 1 of the phenotypic changes that reflect abnormalities in myelination.^{15,18,23} In this study, we assess this aspect of injury in mouse sciatic nerves which were dounced and lysed in immunoprecipitation buffer comprised of 10 mM Tris-HCl [pH 7.5], 5 mM EDTA, 1% Nonidet P-40, 0.5% deoxycholate, 150 mM NaCl and supplemented with protease inhibitors. The lysates were microcentrifuged at 13000g for 15 minutes. The pellet formed harbors the insoluble material containing hydrophobic aggresomes, which was then incubated with 10 mM Tris-HCl, 3% SDS for 10 min at room temperature, then sonicated for 20 seconds at an amplitude of 30% (Optic Iyemen System). The total protein concentrations were measured using the Lowry Protein Assay and then used for Western Blot analysis in equal amounts. The appearance of signals of a higher molecular weight than non-aggregated PMP22 proteins in the insoluble fractions is indicative of PMP22 aggresomes formation.

Statistical Analysis

Data analysis was performed using GraphPad Prism 6. Statistical significance was assessed by 1 way ANOVA Tukey's post-test for multiple comparisons. Data are presented as mean \pm standard error from multiple independent experiments. *P* value \leq .05 was considered significant. The (*) symbol is used to denote significance when comparing non-treated diabetic or treated-diabetic groups versus (vs) the control group. While the (#) symbol was used to denote significance when comparing treated-diabetic groups versus (vs) the diabetic non-treated group.

Results

Effect of HET0016 Administration on the Glycemic Indices of MKR Non-Obese T2DM Mice

FVB controls, MKR or MKR mice treated with the specific 20-HETE synthase and/or CYP4A inhibitor, HET0016 for 10 weeks were monitored for fluctuations in body weight and glucose levels (to assess progression of hyperglycemia) throughout the entire study as well as circulating insulin and Hb_{A1C} levels upon sacrifice. A significant increase in glycated hemoglobin levels and an

Table 1. Metabolic Characteristics

GROUP	N	HbA1c (%)	CIRCULATING INSULIN (NG/ML)	BODY WEIGHT (G)
FVB-Control	11	5.1 ± 0.1	1.03 ± 0.1	30.9 ± 0.5
MKR-Diabetic	11	8.26 ± 0.3*	4.53 ± 0.4*	28.8 ± 0.9
MKR-Diabetic + HET0016	11	8.04 ± 0.23*	4.51 ± 0.4*	28.6 ± 0.4†

NOTE. Terminal body weights, glycated hemoglobin (HbA1c) and serum circulating insulin levels in FVB control mice and T2DM MKR mice. T2DM MKR mice were treated with HET0016 (2.5 mg/kg) for 10 weeks. Values are the means ± SEM.

* $P < .05$, vs control.

† $P < .05$, vs diabetic.

increase in circulating insulin levels were observed in tandem with the development of hyperglycemia in diabetic animals compared to the control group (Table 1), with no change in body weight. Interestingly, HET0016 administration did not have any significant effect on the glycemic index, or insulin resistance of the diabetic animals (Table 1). These results suggest that the effect of HET0016, if observed, is independent from any glucose regulating effect.

CYP4A Inhibition Attenuates Sensory and Motor Deficits in MKR Non-Obese T2DM Mice

DPN often courses with positive symptoms such as pain, or negative symptoms such as sensory loss and weakness.⁴¹ To investigate the role of HET0016 in diabetes-induced nerve dysfunction, we examined various sensory and motor modalities of the peripheral nerve in the FVB controls, MKR or MKR mice treated with HET0016, via a series of neurophysiological and behavioral tests. In our preliminary assessment, FVB control mice were either treated with vehicle or with HET0016, and motor nerve conduction velocity (MNCV) and sensory nerve conduction velocity (SNCV) were recorded. No significant changes were observed between vehicle treated FVB controls and FVB control mice treated with HET0016 in both MNCV (42.22 ± 0.29 vs 39.54 ± 0.64) and SNCV recordings (28.68 ± 0.24 vs 27.17 ± 0.16) respectively. Consequently, the HET0016-treated FVB control was not included in the rest of the study. By contrast, our NCV measurements reflect a decrease in sensory and motor conduction in the MKR diabetic animals compared to their FVB controls. By contrast, NCV readings in the HET0016-treated group show significant neurophysiological improvements relative to the diabetic group (Fig 1 A, B). We further assessed sensory nociceptive changes based on negative symptoms. We predicted that mice with no peripheral nerve injury are capable of thermal sensation compared to animals with diabetes. In the Hind Paw Withdrawal test (Fig 1 C), the results returned from the MKR diabetic mice show an increased withdrawal latency that achieved statistical significance by contrast to their FVB controls. Interestingly, HET0016-treated MKR mice had a significantly lower latency suggesting that the treatment alleviated deficits in thermal pain perception. Further, we examined neuromuscular

strength via the Grip Strength test. MKR animals exhibit a reduced latency to fall indicative of compromised motor function. By contrast, MKR animals treated with HET0016 performed with significantly increased strength compared to the untreated MKR mice (Fig 1 D). Moreover, sensorimotor dysfunction was assessed by the Raised Beam Walking test. Testing results show MKR diabetic animals to perform the test over a longer period of time (Fig 1 E) owing to a significantly reduced speed (Fig 1 F) while crossing the beam with an increased tendency to stop (Fig 1 G) and slip (Fig 1 H) compared to the FVB controls that seemed to perform with minimal setbacks. Importantly, HET0016-treated MKR mice exhibit a significantly improved performance compared to diabetic MKR mice. (Fig 1 A-H). Taken together, these results indicate that HET0016 treatment was effective in restoring sensorimotor coordination in type 2 diabetic animals.

CYP4A Inhibition Normalizes Diabetes-Induced Alterations in Myelin Sheath key Components in Sciatic Nerves of MKR Non-Obese T2DM Mice

To account for the behavioral findings, we examined the molecular impact of HET0016 on the sciatic nerve. Peripheral Myelin Protein (PMP22) and Myelin Protein Zero (MPZ) are essential myelin proteins central to maintaining the integrity and compaction of the peripheral myelin sheath. PMP22 and MPZ were assessed as markers of peripheral nerve injury. Western blot analysis shows a significantly altered expression in the sciatic nerves of the MKR mice in both myelin proteins compared to their control littermates (Fig 2 A, B). Interestingly, HET0016 administration to MKR mice significantly restored myelin protein levels close to controls. We further assessed the molecular status of aggregate prone PMP22 proteins by the Aggregation Assay. The results reflect a phenotypic marker of myelin abnormality in which PMP22 proteins of a higher molecular weight in sciatic nerves from diabetic animals than wild-type, non-aggregated PMP22 proteins compared to controls. This is indicative of the formation of PMP22 heterodimers in the insoluble fraction assessment of the lysates. By contrast, lysates from the HET0016-treated group exhibit a reduction in aggregates formation.

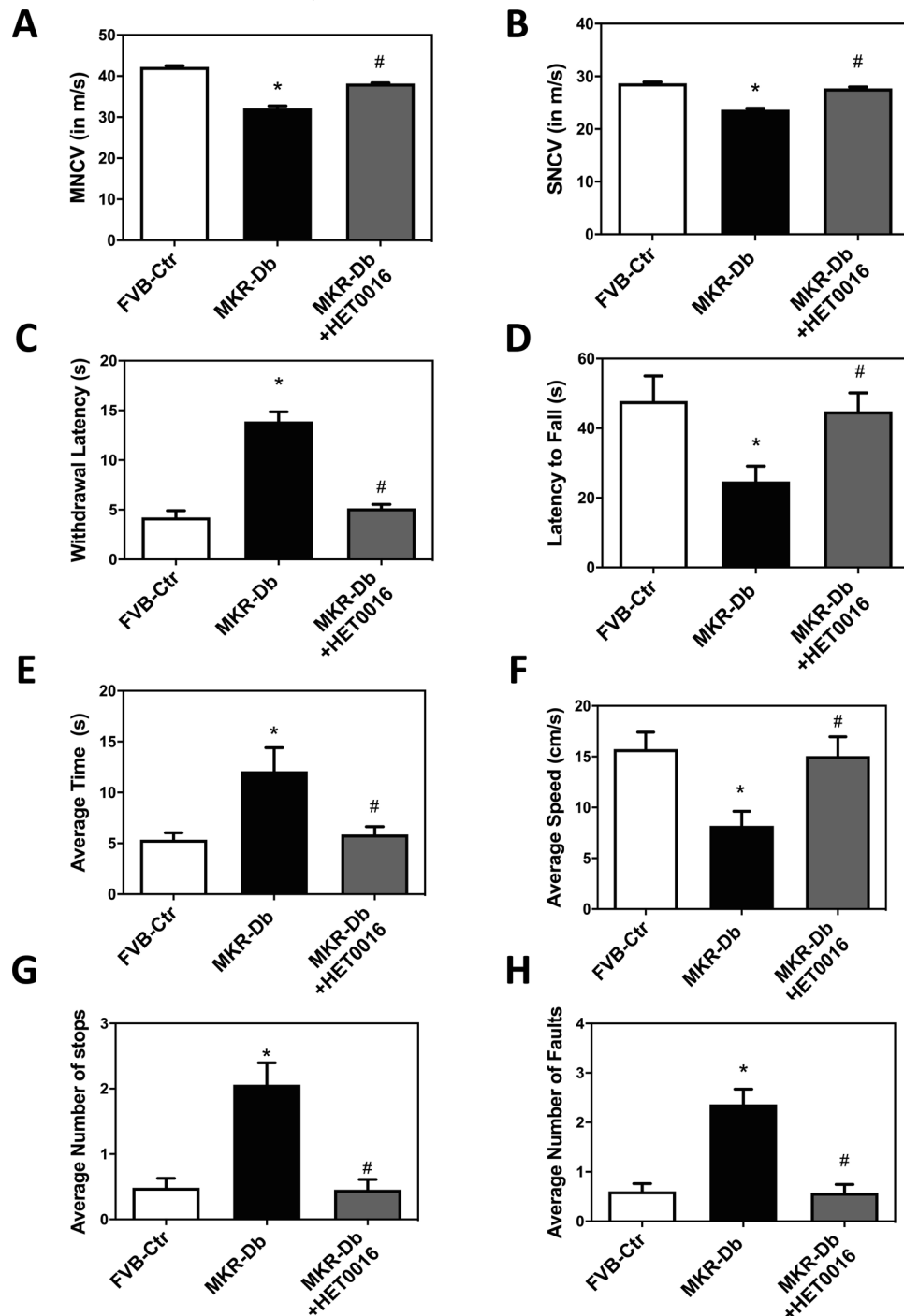


Figure 1. HET0016 administration attenuates behavioral sensory and motor deficits observed in MKR non-obese type 2 diabetic mice. Diabetes brings about nerve impairments in diabetic subjects. We performed behavioral and functional assessments to phenotype neuropathy in the animal groups prior to sacrifice and after 10 weeks of HET0016 administration, respectively. Histograms representing (A) Motor and (B) Sensory nerve conduction velocities ($n = 5$). Histograms representing (C) nociception latencies assessed by Thermal Hind Paw Withdrawal test ($n = 11$) latencies reflecting (D) neuromuscular strength assessed by the Grip Strength Test ($n = 11$) and (E-H) fine sensorimotor coordination assessed by the Raised Beam Walking Test ($n = 11$). Histograms represent average time (E), speed (F) stops (G) and foot faults (H). Values are the means \pm SEM. * $P < .05$, versus control. # $P < .05$, versus MKR.

Together, the data show PMP22 proteins to be aggregated in sciatic nerves of MKR mice by contrast to controls and HET0016-treated animals whereby PMP22 aggregation is attenuated (Fig 2C). These findings suggest that myelin protein abnormalities observed in MKR non-obese T2DM mice, which are quelled upon HET0016 administration.

HET0016 Alleviates Peripheral Nerve Injury by Restoring CYP4A-Induced Oxidative Stress in Sciatic Nerves of MKR Non-Obese T2DM Mice

We further set out to explore the mechanism of action with which HET0016 attenuates peripheral

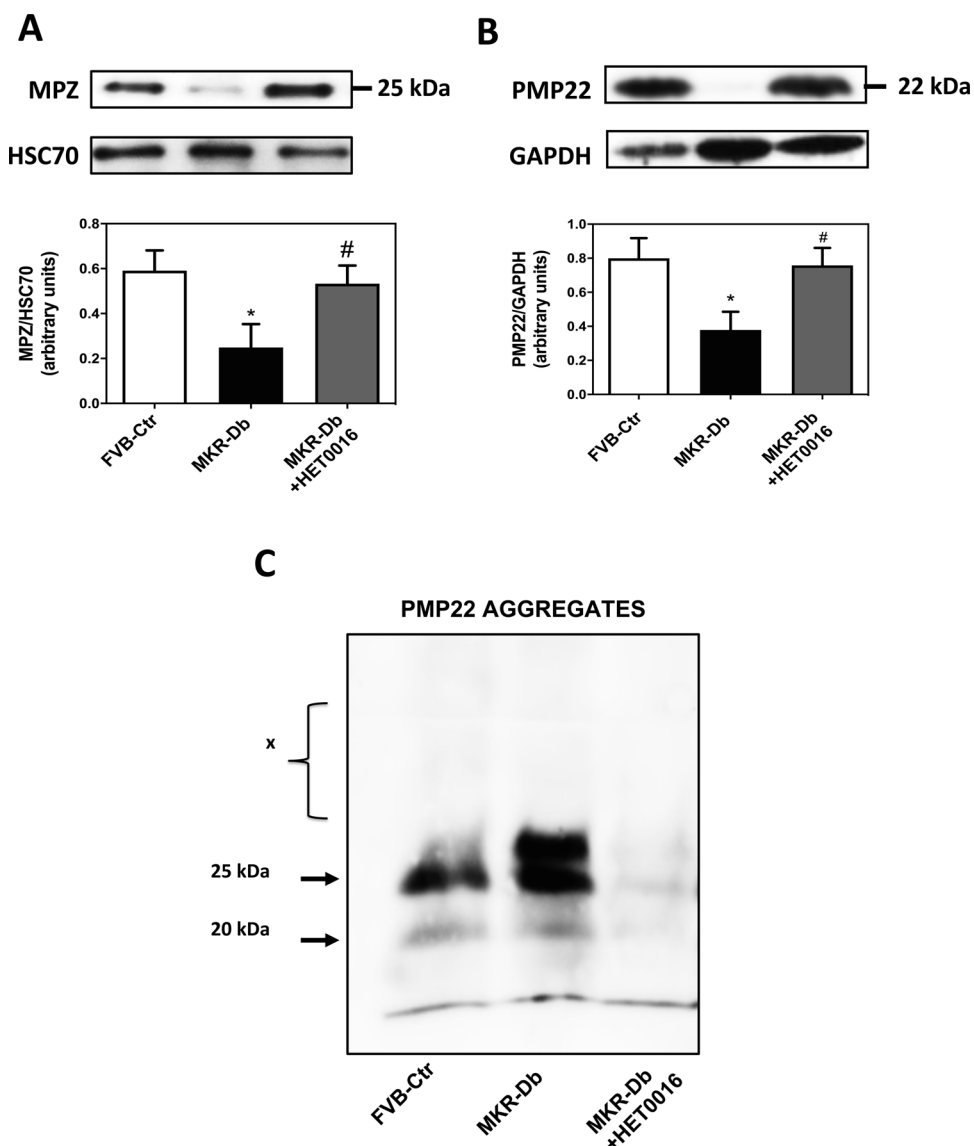


Figure 2. HET0016 administration intercepts diabetes-induced alterations in MPZ and PMP22 myelin protein profiles in the sciatic nerve of MKR non-obese type 2 diabetic mice. Myelin protein soluble and insoluble profiles were assessed via western blot in sciatic nerves isolated from FVB control mice, MKR non-obese type 2 diabetic mice, and MKR non-obese type 2 diabetic mice treated with HET0016. Representative western blots with their respective densitometric quantification are shown for (A) MPZ ($n = 5$) and (B) PMP22 ($n = 5$). (C) Putative western blot of the insoluble, high molecular PMP22 aggregates indicated by x. MKR non-obese type 2 diabetic mice exhibit PMP22 heterodimers of a higher molecular weight compared to controls. HET0016 treatment attenuates the formation of PMP22 heterodimers. Values are the means \pm SEM. * $P < .05$, versus control. # $P < .05$, versus MKR.

nerve injury. HET0016 is a selective CYP4A inhibitor. We thus assessed the CYP4A protein levels in sciatic nerve lysates, and the findings show a basal expression of CYP4A in control animals which was significantly increased in diabetic animals. HET0016 treatments significantly reduced CYP4A expression levels indicative of its inhibitory effect (Fig 3A). Concurrent with CYP4A overexpression in MKR animals, we measured 20-HETE levels to correlate the underlying activity of CYP4A. The results show a significant rise in 20-HETE production in the sciatic nerves of the MKR mice in parallel to increased CYP4A expression (Fig 3B). The efficiency of HET0016 was further validated whereby 20-HETE levels in sciatic nerves of MKR treated animals with HET0016 was significantly reduced compared to diabetic animals (Fig 3B). Together, the data suggest that peripheral

nerve injury may be mediated through a CYP4A-dependent mechanism.

To further dissect the oxidative status of the peripheral nerve, cellular H_2O_2 and superoxide production were measured in sciatic nerves via DHE staining and HPLC, respectively. Sciatic nerve sections were visualized by DHE staining (Fig 3C, D) and analyzed by HPLC (Fig 3E) which showed a significant increase in intracellular ROS production in the MKR mice compared to their control littermates, and this was significantly reduced upon HET0016 treatment. Moreover, CYP450 enzymes have been reported to be associated with an NADPH subunit.^{14,58} NADPH oxidase activity correlates with a direct measure of superoxide anion production. As expected, the data show that superoxide anion production significantly increased in diabetic animals in

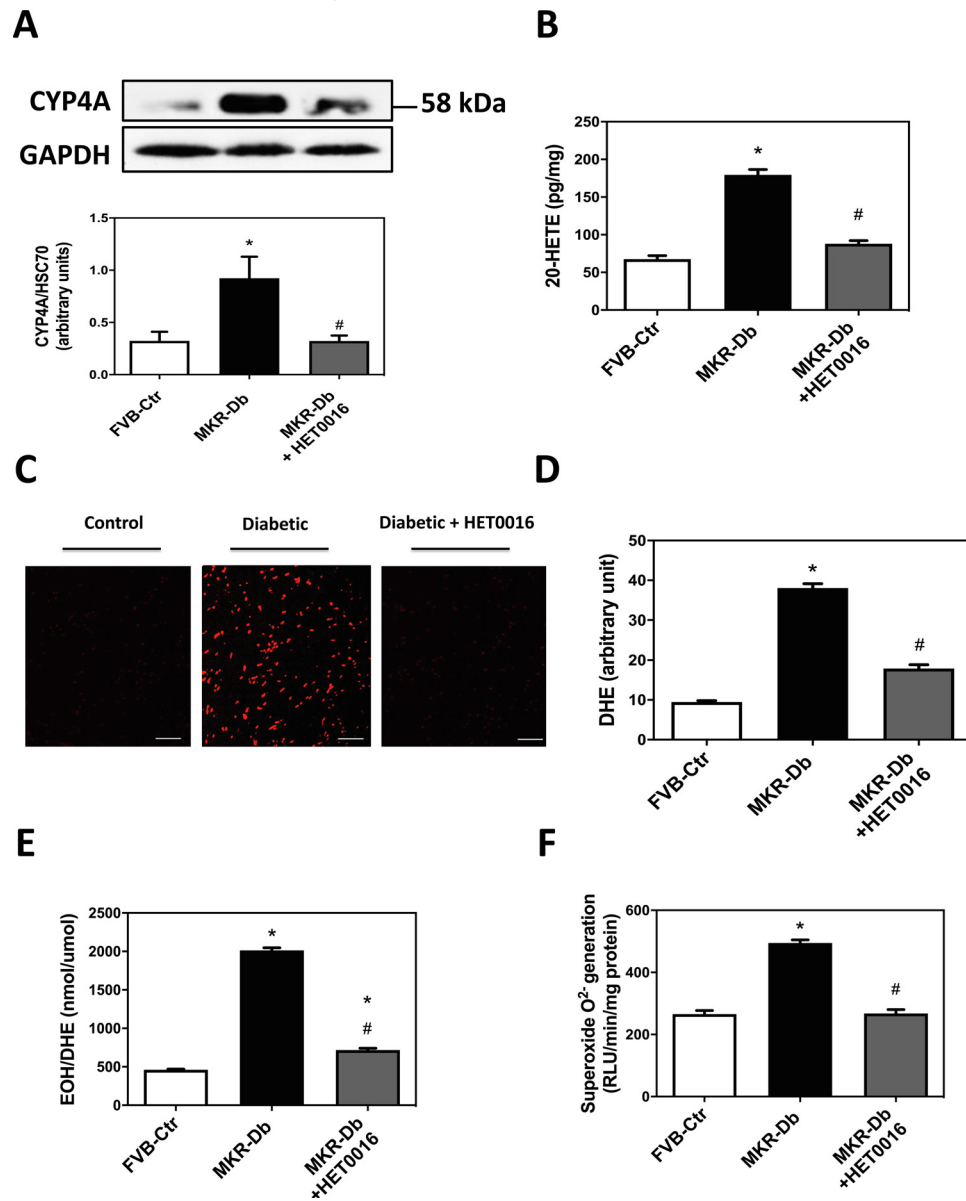


Figure 3. HET0016 administration attenuates diabetes induced, CYP4A-dependent ROS and 20-HETE overproduction in sciatic nerves of MKR non-obese type 2 diabetic mice to homeostatic levels. Diabetes is associated with ROS overproduction which we assessed in sciatic nerves isolated from FVB control, MKR non-obese type 2 diabetic mice and MKR non-obese type 2 diabetic mice treated with HET0016. Sciatic nerves lysates were first examined for CYP4A expression and activity. (A) Representative western blot of CYP4A expression with the respective densitometric quantification ($n = 5$). CYP4A activity was reflected by assessment of endogenous (B) 20-HETE production via HPLC analysis ($n = 5$). (C) Representative images of ROS production assessed by DHE staining and the corresponding (D) quantification of ($n = 5$) using the Image-Pro Plus 4.5 software. (E) Assessment of superoxide generation in sciatic nerves via HPLC analysis ($n = 11$) (F) Histogram representative of NADPH-induced ROS generation ($n = 5$). Values are the means \pm SEM. * $P < .05$, versus control. # $P < .05$, versus MKR.

comparison to their controls and is significantly reduced upon HET0016 treatment (Fig 3F). These findings suggest that sciatic nerve injury is correlated with an increase in ROS production through an NADPH-dependent pathway.

Hyperglycemia Alters Autophagic Defenses and AMPK Signaling in Sciatic Nerves of MKR Non-Obese T2DM Mice

Next, we sought to understand whether CYP4A inhibition impacts central cellular processes associated with

myelin protein maintenance. For instance, autophagic processes are significant cellular defenses for the restoration of homeostasis, recycling nutrients or tagging cargo for lysosomal degradation. Defects in autophagy machinery are shown to be associated with various disorders, with prominent contribution to protein misfolding.^{6,18,22,23,38} Consequently, in order to correlate the observed alterations in myelin protein profiles and PMP22 aggregation, we next assessed protein levels of central autophagy orchestrators. Our data show a significant increase in the key regulators of autophagy, Beclin-1, expression in sciatic nerves of the MKR mice relative to their controls, and a restoration of Beclin-1

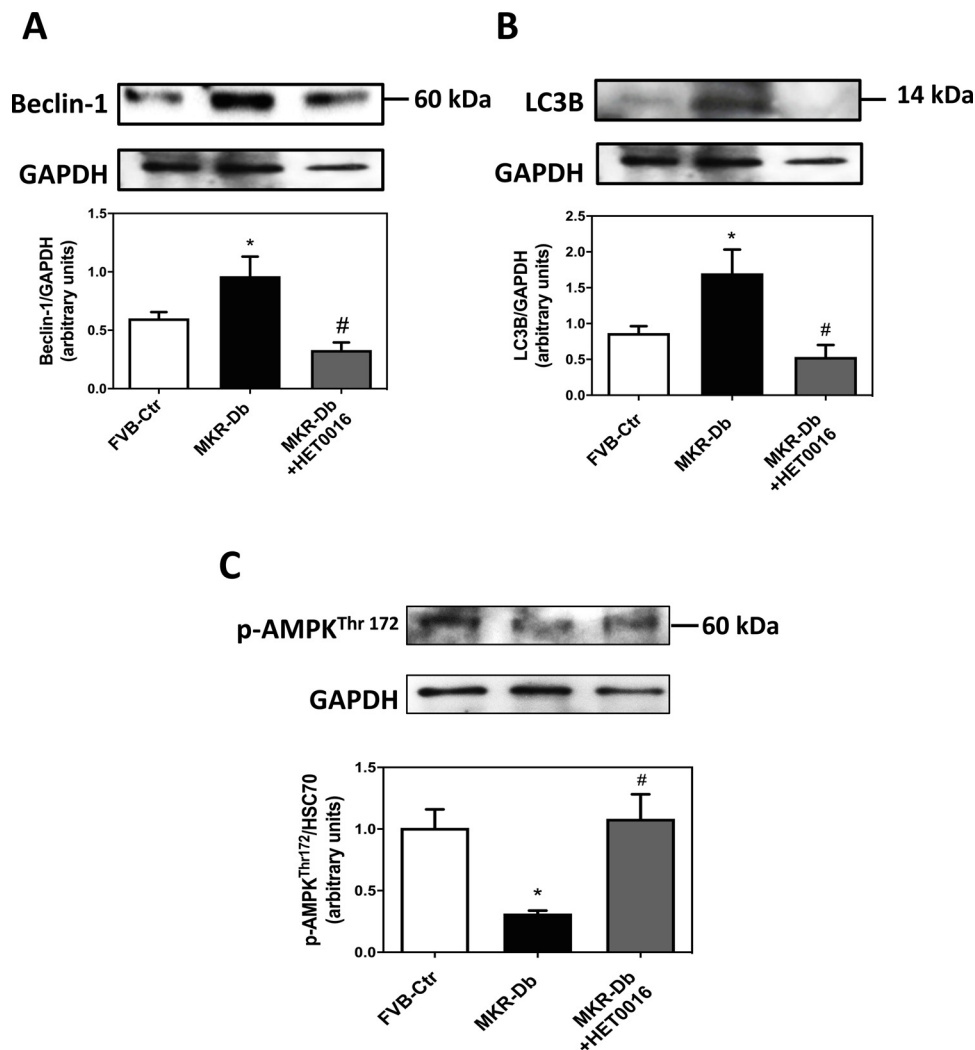


Figure 4. HET0016 administration attenuates diabetes-induced alterations in autophagic response markers and AMPK signaling in sciatic nerves of MKR non-obese type 2 diabetic mice. Key autophagy protein expression was examined in sciatic nerve lysates from FVB control mice, MKR non-obese type 2 diabetic mice, and MKR non-obese type 2 diabetic mice treated with HET0016. Representative western blots with the respective densitometric quantification are shown for (A) Beclin-1 (n = 5), (B) LC3B (n = 5) (C) p-AMPK^{Thr172} (n = 5). Values are the means \pm SEM. * $P < .05$, versus control. # $P < .05$, versus MKR.

upon HET0016 administration (Fig 4A). We further examined LC3B indicative of autophagosome recruitment and formation.⁵⁶ LC3B protein expression was significantly elevated in the sciatic nerve of the MKR mice by contrast to the controls, whereas HET0016-treated MKR mice exhibit reduced LC3B levels (Fig 4B).

Moreover, the metabolic perturbances brought about by diabetes have been reported to trigger the alteration of signaling cascades culminating in organ and tissue injuries. In addition to that, AMPK is a known key regulator of autophagy.³⁰ In order to cross-correlate the molecular findings and further delineate the mechanisms at play in the pathogenesis of DPN in T2DM, we next assessed AMPK phosphorylation (p-AMPK). p-AMPK^{Thr172} protein expression, indicative of AMPK pathway activation, was significantly reduced in MKR mice relative to the expression observed in the FVB control mice. HET0016 administration restored p-AMPK^{Thr172} protein expression to levels close to that observed in the control FVB mice (Fig 4C).

These findings are suggestive of significant alterations in autophagosome recruitment and activity which may mediate the underlying neurological pathology. Furthermore, these results also suggest a potential role of AMPK in inducing peripheral nerve injury. Therefore, we assessed if AMPK activation halts diabetes-induced peripheral nerve injury, since its role, and to our knowledge is not yet described.

Effect of Metformin Administration on the Glycemic Index of MKR Non-Obese T2DM Mice

10 weeks of age FVB control mice, MKR non-obese T2D mice and MKR non-obese T2D mice treated with metformin, an AMPK activator were used. Mice body weight, random blood glucose levels and glycemic index (HbA1c) were monitored throughout the study. The results show no significant differences in body weight among the groups, however there was a significant

Table 2. Metabolic Characteristics

GROUP	N	HbA1c (%)	CIRCULATING INSULIN (NG/ML)	BODY WEIGHT (G)
FVB-Control	10	5.18 ± 0.1	0.93 ± 0.03	31.5 ± 0.7
MKR-Diabetic	11	8.25 ± 0.2*	4.5 ± 0.1*	30.3 ± 1.1
MKR-Diabetic + Metformin	11	6.96 ± 0.2*,†	3.49 ± 0.1*,†	29.3 ± 0.9

NOTE. Terminal body weights, glycated hemoglobin (HbA1c) and serum circulating insulin levels in FVB control mice and T2DM MKR mice. T2DM MKR mice were treated with Metformin (150 mg/kg) daily for 13 weeks. Metformin activates AMPK signaling through targeting hepatic mitochondrial respiratory chain inhibition to restore insulin sensitivity.⁴⁴ Values are the means ± SEM.

**P* < .05, vs control.

†*P* < .05, vs diabetic.

difference in HbA1c and circulating insulin levels of diabetic animals compared to the control littermates. However, it is noteworthy to mention that Metformin administration showed a significant reduction in the glycemic index and circulating insulin of the diabetic treated animals compared to the diabetic non-treated group, verifying its anti-hyperglycemic effect. Nonetheless, these levels remained significantly higher than the controls group (Table 2).

Metformin Administration Corrects Neural Sensory and Motor Abnormalities in MKR Non-Obese T2DM Mice

To investigate the role of AMPK activation in diabetes-induced nerve dysfunction, we examined various sensory and motor modalities of the peripheral nerve in our murine model via a series of behavioral tests. We initially measured the sensory nocifensive responses of the animals via the Hind Paw Withdrawal test (Fig 5A). The data show the development of thermal hypoalgesia in the MKR mice reflected by a significantly increased withdrawal latency relative to the FVB controls. Interestingly, MKR mice treated with Metformin had a significantly lower latency suggesting that Metformin restored thermal pain perception. We next examined neuromuscular strength via the Grip Strength test. MKR mice exhibit a reduced latency to fall indicative of compromised motor function, which was restored in Metformin-treated MKR mice (Fig 5B). To further correlate sensory and motor dysfunction, findings from the Raised Beam Walking test show an overall poor performance by the MKR non-obese T2D mice. These mice took a significantly longer period of time to complete the test (Fig 5C) with a reduced speed (Fig 5D) and an increased tendency stop (Fig 5E) and to slip (Fig 5F). By contrast, Metformin-treated MKR mice exhibited a performance similar to the FVB control group (Fig 5A-F). The results of this test indicate that Metformin treatment improved the peripheral neuropathy-associated deficits in the MKR non-obese T2D mice.

We also examined the molecular impact of Metformin on the most essential myelin proteins, MPZ, central to maintaining the integrity and compaction of the peripheral myelin sheath. Western blot analysis of sciatic nerve lysates shows a significantly altered expression of MPZ

in diabetic mice compared to the controls (Fig 6A). Interestingly, Metformin-treated MKR mice exhibit a restoration of MPZ levels close to control levels.

Metformin Blunts Diabetes-Induced Oxidative Stress and Peripheral Nerve Injury in MKR Non-Obese T2DM Mice

We next quantified 20-HETE metabolite levels to assess the effect of Metformin on the underlying activity of CYP4A. The results show a significant rise in 20-HETE production in the sciatic nerves of the MKR mice compared to FVB controls. By contrast, Metformin-treated MKR mice exhibit a slight, but significantly reduced 20-HETE levels compared to MKR non-treated animals (Fig 6B). However, 20-HETE levels remained significantly elevated in Metformin-treated MKR mice relative to the FVB controls (Fig 6B). We further examined if Metformin treatment can regulate hyperglycemia-induced ROS production. For that, sciatic nerve sections were analyzed by HPLC to assess superoxide generation (Fig 6C). Results show a significant increase in intracellular ROS production in MKR mice compared to their control FVB littermates, and this was significantly reduced upon Metformin treatment. Moreover, NADPH-dependent ROS production was assessed in sciatic nerves of mice via the NADPH-oxidase assay. The data show that superoxide anion production significantly increased in the MKR mice in comparison to the controls and is significantly reduced upon Metformin treatment (Fig 6D). These findings suggest that sciatic nerve injury and MPZ protein alteration is correlated with an increase in ROS production through an NADPH-dependent mechanism.

Metformin Alleviates Autophagy Protein Alterations Triggered by Hyperglycemia in the Sciatic Nerve of MKR Non-Obese T2DM Mice

In the same spirit of our previous findings (Fig 4A-B), we next examined if AMPK activation normalizes the key proteins Beclin-1 and LC3B as markers of the autophagic response in sciatic nerves of the MKR non obese T2DM mice. We were interested in examining these proteins in the context of intact tissue and visualize their expression throughout the tissue compartments or cell types. Immunohistochemical analysis of sciatic nerve

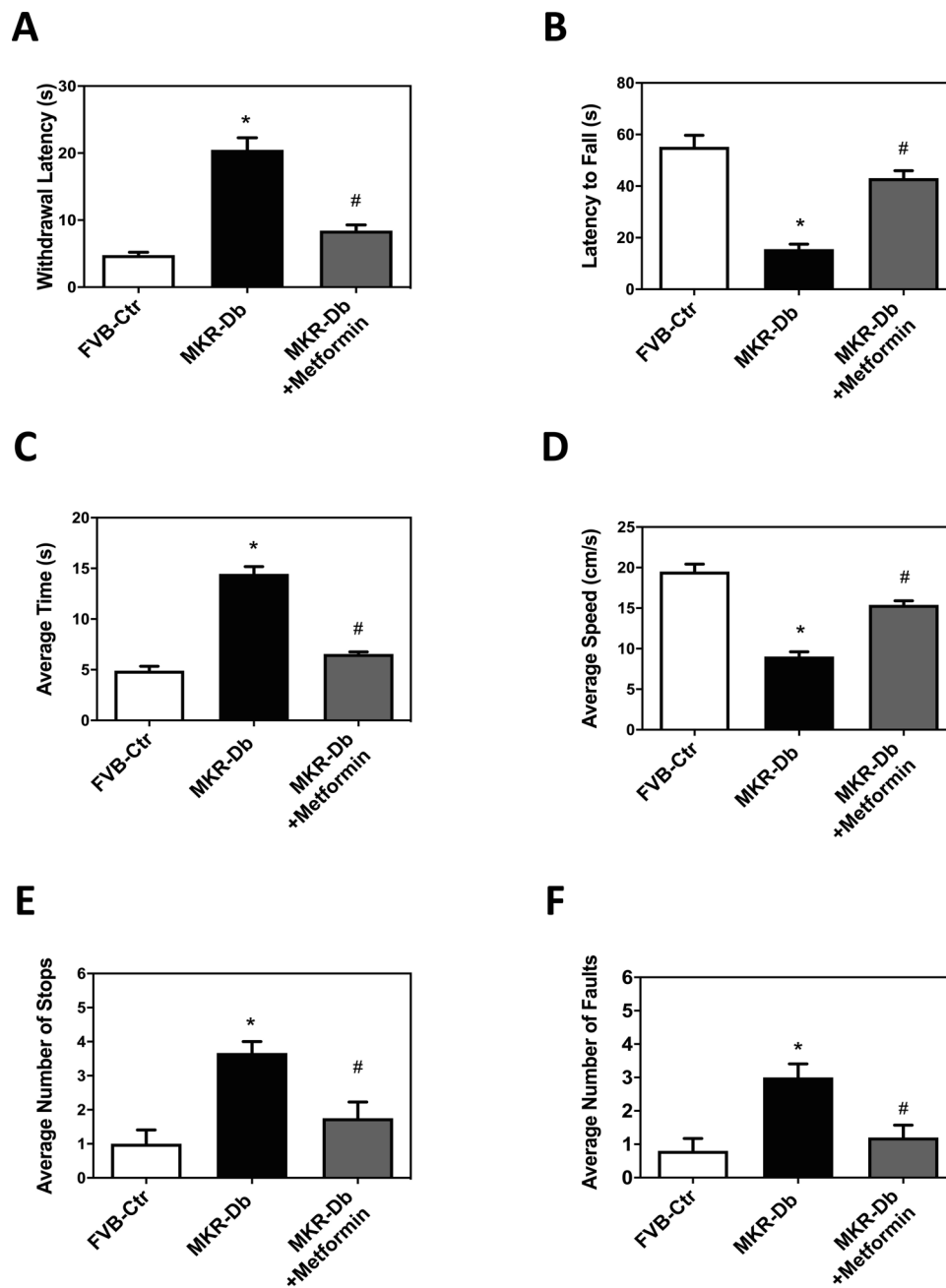


Figure 5. Treatment with Metformin abates sensorimotor deficits in MKR non-obese type 2 diabetic mice. Diabetes is often associated with abnormalities in sensory and motor neural functions. We examined the behavioral performance of FVB control mice, MKR non-obese type 2 diabetic mice, and MKR non-obese type 2 diabetic mice treated with HET0016, in a series of tests to phenotype neuropathy. Histograms representing (A) thermal sensitivity to pain assessed by Thermal Hind Paw Withdrawal test ($n = 5$) and (B) latencies reflecting neuromuscular strength assessed by the Grip Strength Test ($n = 5$) in addition to (C-F) fine motor coordination and gait assessed by the Raised Beam Walking Test ($n = 5$). Values are the means \pm SEM. * $P < .05$, versus control. # $P < .05$, versus MKR.

sections show a significant increase in Beclin-1 and LC3B expression in sciatic nerves of MKR mice relative to the controls, and their respective attenuation in Metformin-treated MKR mice (Fig 7A-D).

Discussion

DPN is a common diabetic complication with autonomous onset and characteristic nerve abnormalities^{15,60} despite proper management of the disease. Consequently,

the largest clinical trials urged the need for novel approaches to the management of DPN.

Oxidative stress is a major mediator of diabetic complications^{12-14,36,39} including DPN.^{15,23} Yet, treatment with antioxidants have not demonstrated maximal therapeutic potential.^{26,40,46,48} Therefore, identifying ROS sources playing a role in the pathogenesis of DPN could be a potential approach in treating DPN. Accordingly, we investigate CYP450 enzymes as potent sources of ROS in DPN. This study provides evidence that

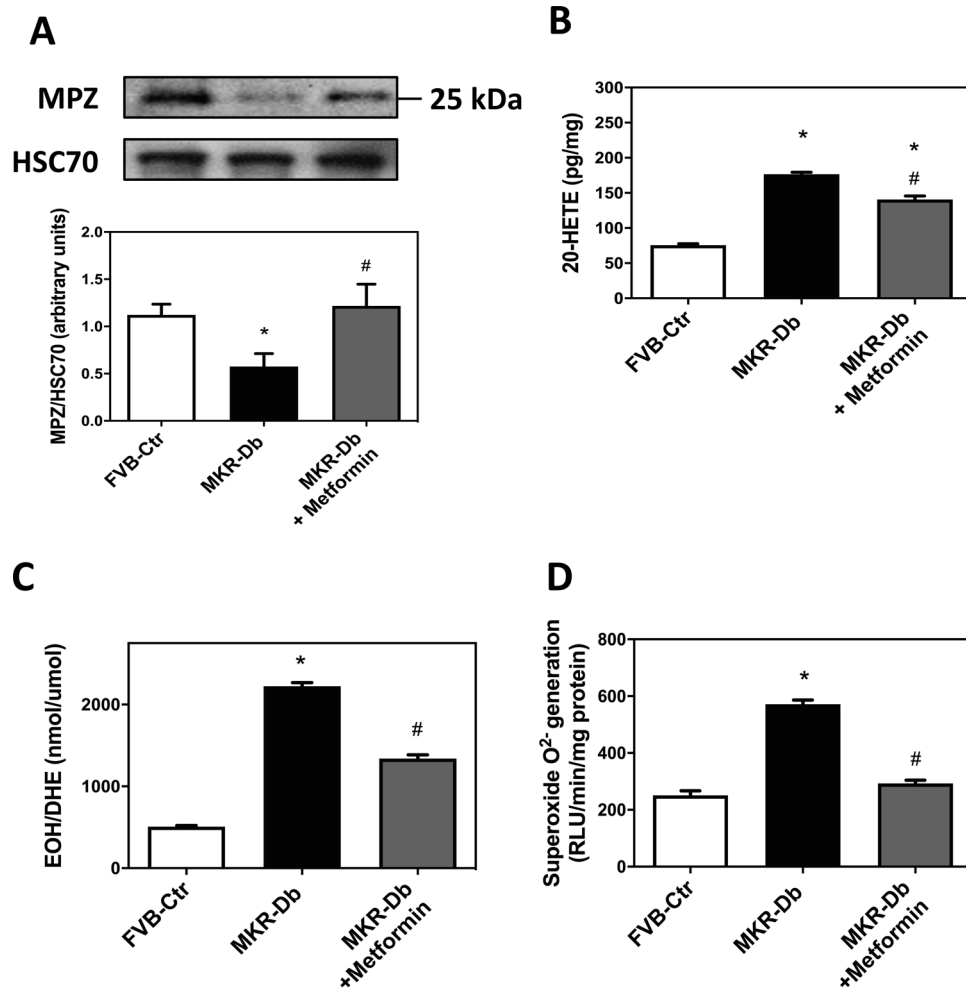


Figure 6. Metformin administration reduces peripheral nerve injury and NADPH-derived ROS production in MKR non-obese type 2 diabetic mice. Sciatic nerves were isolated from FVB control, MKR non-obese type 2 diabetic mice and Metformin-treated MKR non-obese type 2 diabetic mice. MPZ, the predominant myelin protein of the peripheral nerves, was assessed in sciatic nerve lysates as a marker of peripheral nerve injury. Representative western blot and respective densitometric quantification is shown for (A) MPZ ($n = 5$). (B) 20-HETE production via HPLC analysis ($n = 7$). Diabetes-associated superoxide anion production was measured by (C) HPLC ($n = 5$) and (D) NADPH oxidase Activity Assay ($n = 5$). Values are the means \pm SEM. * $P < .05$, versus control. # $P < .05$, versus MKR.

hyperglycemia impacts peripheral nerve integrity through the generation of ROS by CYP4A enzymes. We highlight the 20-HETE synthase inhibitor HET0016, as a possible pharmaceutical approach to treat DPN.

We first investigated the role of CYP4A in MKR T2DM mice. Sciatic nerve tissues from diabetic mice show increased CYP4A protein expression and 20-HETE production. This was concurrent with decreased MPZ and PMP22 protein expression. The observed decrease in MPZ is consistent with other studies showing that diabetes alters SCs myelin protein expression.^{5,15} Of note any alteration in myelin protein of the SCs is associated with nerve dysfunction. DPN has been dubbed a complex disease in both T1D and T2D with overlapping clinical manifestations, but distinct underlying mechanistic insults.¹⁶ Additionally, abnormalities in PMP22 proteins were observed in insoluble fractions of sciatic nerves of diabetic animals. Diabetic animals exhibited increased accumulation of aggregated PMP22 proteins in our study, supporting previous studies that linked both protein misfolding and myelin injury in diabetes.^{15,23} These findings were reflected by behavioral

assessments where diabetic animals exhibited poor locomotion, neuromuscular strength, and nociception, and paralleled by reduced sensory and motor NCVs from diabetic animals. The obtained findings in diabetic animals mimic the clinical presentation of diabetic subjects, verifying the neuropathic phenotype in our animal model.³ However, future investigations are warranted to assess mechanical sensitivity as an additional modality affected in DPN with a prolonged duration of diabetes onset. Moreover, the data support the notion that myelin protein alterations have deleterious effects on the functional integrity of peripheral nerves.^{5,15,24} The results are in accordance with other studies that associate alterations in myelin protein profiles with neurodegenerative anomalies.¹⁸ Interestingly, the inhibition of 20-HETE synthase restored myelin and neurological defects in diabetic animals, while inhibition in FVB controls did not show any significant change relative to vehicle-treated controls. Taken together, the results highlight the possible involvement of 20-HETE in peripheral nerve injury in diabetes and dysmyelination.

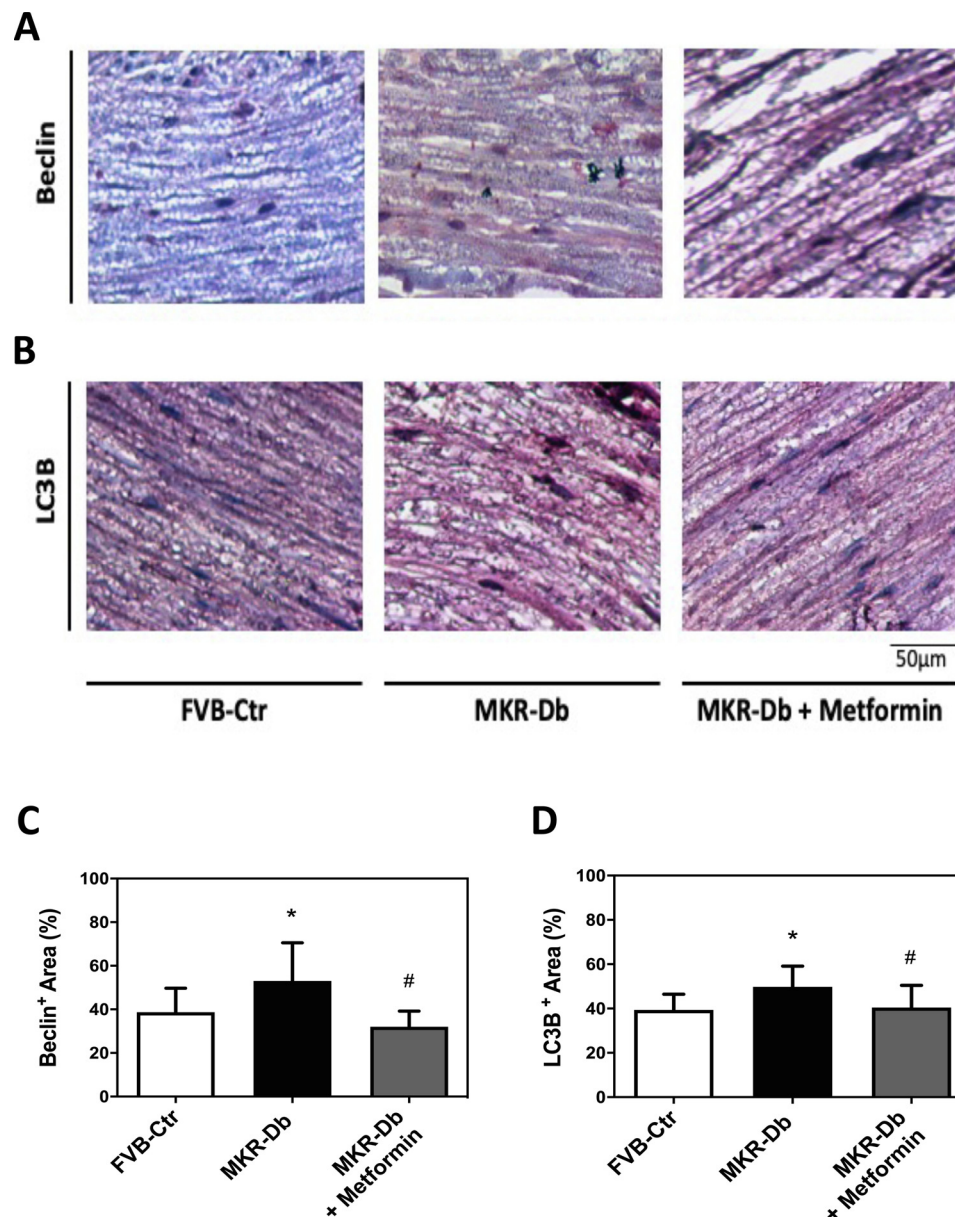


Figure 7. Diabetes-induced canonical autophagy in sciatic nerves is restored upon Metformin treatment in MKR non-obese type 2 diabetic mice. Longitudinal sections of sciatic nerves were examined for protein markers of autophagy. Representative immunohistochemistry images of sciatic nerves of FVB control, MKR non-obese type 2 diabetic mice and MKR non-obese type 2 diabetic mice treated with Metformin stained with (A) Beclin-1 and (B) LC3B with their respective quantifications (C, D). Values are the means \pm SEM (n = 5). * $P < .05$, versus control. # $P < .05$, versus MKR.

CYP4A and 20-HETE levels were significantly increased in diabetic animals reflecting elevated CYP4A activity that was restored upon HET0016 administration. Compounding this observation, it has been shown that 20-HETE mimics TRPV1 channel agonists of sensory neurons, associated with thermal hyperalgesia.⁵⁴ In our study, HET0016-treated diabetic animals demonstrated improved sensorimotor function and nociception compared to the diabetic group. This is of significance as the bio efficacy of HET0016 as a therapeutic agent may be multifaceted and warrants investigation of 20-HETE-dependent activation of TRPV1 channels in DPN. On another note, given our behavioral and electrophysiology data, the DPN phenotype in our murine model parallels intermediary to advanced clinical symptoms of DPN in which loss of sensation is recorded. Besides, 20-

HETE may be an activator of TRPV1 channels in the early painful phase of progression of DPN. Likewise, 20-HETE may be playing a dual injurious role, not just at the neuronal level, but at the vascular level which warrants further investigation such as via the peripheral nerve blood flow assessment.^{25,59}

Besides, previous work correlated CYP4A upregulation induced by hyperglycemia with increased oxidative stress through 20-HETE production leading to injury in kidney tubules and podocytes.^{13,14} The current findings pinpoint CYP4A overexpression in tandem with ROS overproduction. Notably, CYP450 enzymes are associated with a NADPH ROS-producing catalytic center.^{14,58} Our data show increased ROS production and NADPH oxidase activity in the diabetic animals, in validation of oxidative peripheral nerve injury, which was

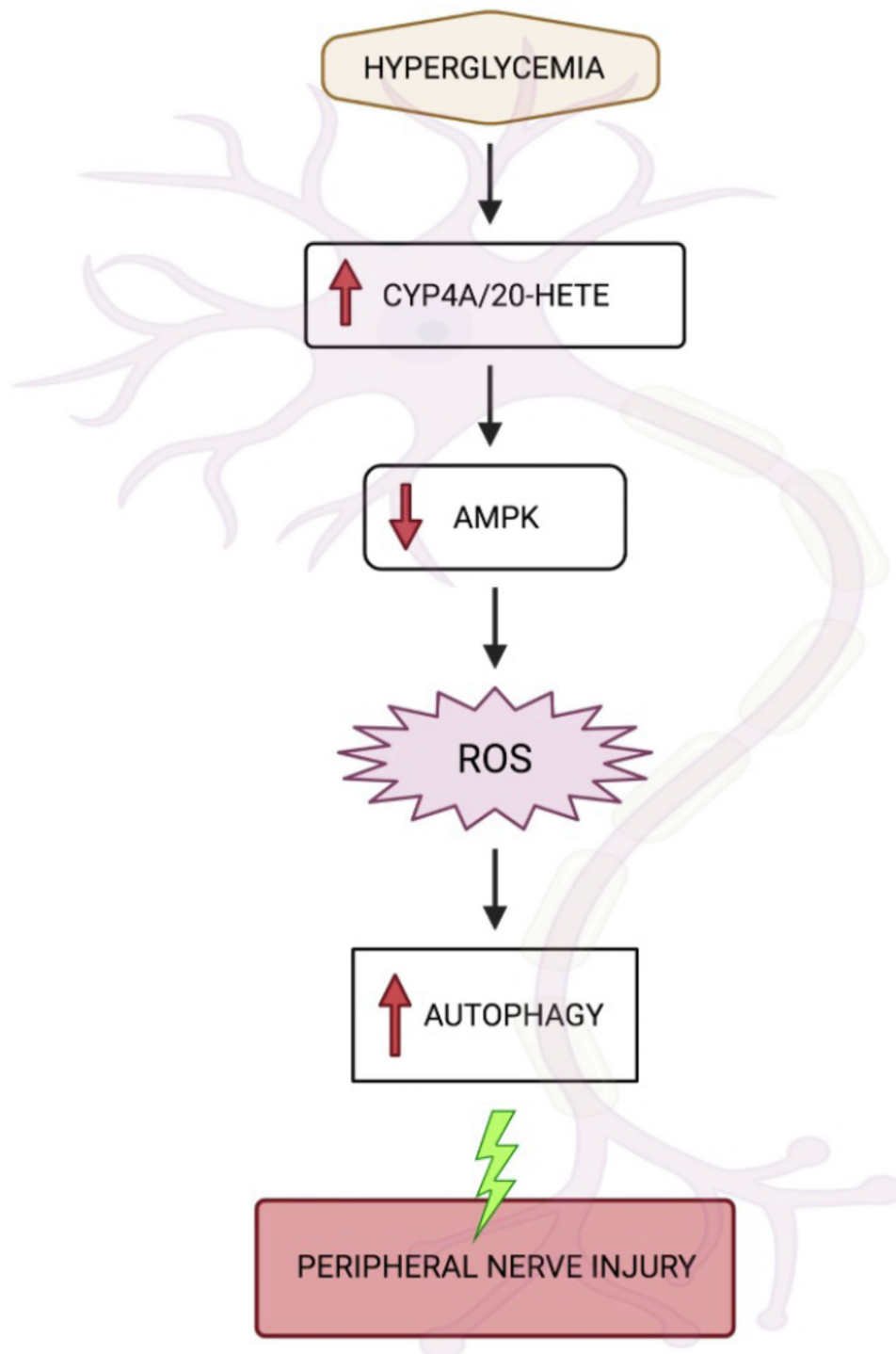


Figure 8. Proposed mechanism of DPN pathogenesis (Figure created with BioRender).

significantly quelled by HET0016. These results underscore the association of CYP4A/20-HETE with increased ROS production through an NADPH-dependent pathway, in line with recent data that verified the role of NADPH oxidase enzymes in the pathogenesis of DPN.¹⁵ Together, we extend the pathological pathway further to CYP4A/20-HETE and pinpoint a potential crosstalk between CYP450 and NADPH oxidase enzymes.¹³

This study also outlined the role of autophagy as a route implicated in hyperglycemia-induced myelin

protein abnormality. Autophagy is linked to various pathologies including diabetes^{6,22,27,56} and neurodegeneration.³⁸ Our results revealed elevated Beclin-1 and LC3B protein expression in diabetic animals, indicative of autophagy activation. Interestingly, HET0016 treatment restored Beclin-1 and LC3B levels which may account for the alleviation of nerve functional changes, suggesting that dysregulated autophagy may contribute to the pathogenesis of DPN. However, the activation of autophagy in our MKR model contrasts with

other studies.⁶ In our work, the activated autophagic responses may be partly due to the development of insulin resistance in our animals¹⁰ On the other hand, autophagy induction may be attributed to damaged protein clearance⁵³ or a transitory phase prior to apoptosis⁶ promoting survival in demyelinating neuropathies.⁴³ While some studies suggest autophagy activation in early stages of injury may be a protective mechanism to trigger recovery and regeneration,²⁷ others correlate it with stress and a trigger for cellular recycling or death.^{18,42} Our findings extend previous work that suggests autophagy activation occurs secondary to nerve injury and oxidative stress.^{27,50}

We next examined AMPK signaling, described to be compromised in diabetes.^{11,39,45} Growing evidence associates AMPK inactivation with oxidative stress^{11,12,33,35,39} while hyperglycemia instills a downregulation of AMPK in various cell types.^{11,12,39,45} Our results show AMPK inactivation corroborating myelin protein disruption and oxidative stress, in accord with others that link AMPK inactivation in DPN to nerve defects, and oxidative injury.^{6,57} More importantly, AMPK is associated with central pathways that modulate autophagy.³⁰ In the NS, AMPK positively modulates neurite development and nerve regeneration^{37,45} and its activation mitigates defective autophagic responses, rescuing SC and peripheral nerve injury in diabetic animals.^{2,6,35} Interestingly, we show AMPK activation following HET0016 administration concomitant with normalized autophagy protein markers in MKR mice. In that manner, HET0016 plays a neuroprotective role, possibly through targeting AMPK. Recent literature associates AMPK activation with reduced eicosanoid production in high-fat diet induced kidney disease.⁸ Whereas 20-HETE-mediated endothelial cell injury was ameliorated upon prolonged AMPK activation.⁵² The current work underscores a previously unreported link between 20-HETE and AMPK in DPN.

To confirm the role of AMPK, we assessed the effect of AMPK activator, Metformin, on peripheral nerve injury. Our findings demonstrate Metformin attenuates the diabetic phenotype of MKR mice and sensorimotor defects, consistent with studies that relate AMPK inactivation to neuronal degeneration and multiple manifestations of DPN.^{2,35,49} Our findings further reflect myelin dysregulation, with a state of oxidative stress in sciatic nerves of diabetic animals that subserve neural defects mitigated by Metformin. These results validate the influence of AMPK on regulating central targets involved in DPN.³⁵ Furthermore, AMPK activation ameliorates NADPH-derived ROS generation in diabetic animals. These results are consistent with studies that show AMPK activation to reduce NADPH oxidase and high glucose-induced ROS production in colorectal cancer cells, and glomerular mesangial cells.^{11,39} Thus, an important finding in this work is that Metformin and HET0016 impact overlapping mechanisms of injury intersecting at oxidative stress, NADPH-derived ROS production, and myelin protein alterations. Our data

further show Metformin to alleviate alterations in autophagy markers in diabetic animals, adding autophagy regulation to the downstream effectors of targeting AMPK. Although Metformin may be closely approximated to hold promise as a therapeutic agent for DPN, there remains a dearth of clinical observations. Interestingly, T2D patients on the receiving end of insulin plus Metformin are reported to be twice as likely to develop diabetic neuropathy.⁷

In this study we highlight the role of 20-HETE in an insulin resistance state independent of obesity. However, elevations in 20-HETE are correlated with other factors such as hypertension, inflammatory disorders, obesity, and insulin resistance¹⁹ that overlap with advanced stages of diabetes. Therefore, additional experiments warrant investigating the identified pathological axis in additional animal models of T2D.

In conclusion, we show that hyperglycemia triggers oxidative injury of the PNS through CYP4A/20-HETE-mediated alteration of AMPK signaling and autophagic defenses. The progression of injury was mediated through compromised myelin protein integrity and peripheral nerve functionality. Inhibiting 20-HETE synthesis demonstrated neuroprotection which may be a novel, multi-targeted approach of clinical significance for the management of DPN. We pinpoint for the first time, a CYP-dependent mechanism of oxidative injury in the pathogenesis of DPN in T2DM. More importantly, we place CYP4A/20-HETE upstream in the pathological axis that contributes to peripheral nerve injury through AMPK inactivation, oxidative stress and autophagic dysregulation (Fig 8).

Author Contributions

AAE conceived and designed the study; MH, performed the experiments and wrote the manuscript; SAE helped in performing some of the experiments and participated to the discussion of the results. MEM; helped in performing part of the experiments; FH, EAS, and SA provided critical scientific input to the experiments. All authors reviewed the results, provided essential reviews of the manuscript, and approved the final version of the paper.

Acknowledgments

We thank the American University of Beirut Animal Care Facility staff for their help in taking care of the animals used in this manuscript. This work was supported by a medical practice plan regular research grant from the American University of Beirut for AAE.

AAE is the guarantor of this study and takes full responsibility for the work as a whole, including the study design, access to data, and the decision to submit and publish the manuscript.

References

- Alaeddine LM, Harb F, Hamza M, Dia B, Mogharbil N, Azar NS, Noureldein MH, El Khoury M, Sabra R, Eid AA: Pharmacological regulation of cytochrome P450 metabolites of arachidonic acid attenuates cardiac injury in diabetic rats. *Transl Res* 235:85-101, 2021
- Atef MM, El-Sayed NM, Ahmed AAM, Mostafa YM: Donepezil improves neuropathy through activation of AMPK signaling pathway in streptozotocin-induced diabetic mice. *Biochem Pharmacol* 159:1-10, 2019
- Biessels GJ, Bril V, Calcutt NA, Cameron NE, Cotter MA, Dobrowsky R, Feldman EL, Fernyhough P, Jakobsen J, Malik RA, Mizisin AP, Oates PJ, Obrosova IG, Pop-Busui R, Russell JW, Sima AA, Stevens MJ, Schmidt RE, Tesfaye S, Veves A, Vinik AI, Wright DE, Yagihashi S, Yorek MA, Ziegler D, Zochodne DW: Phenotyping animal models of diabetic neuropathy: A consensus statement of the diabetic neuropathy study group of the EASD (Neurodiab). *J Peripher Nerv Syst* 19:77-87, 2014
- Brooks SP, Dunnett SB: Tests to assess motor phenotype in mice: A user's guide. *Nat Rev Neurosci* 10:519-529, 2009
- Cermenati G, Abbiati F, Cermenati S, Brioschi E, Volonterio A, Cavaletti G, Saez E, De Fabiani E, Crestani M, Garcia-Segura LM, Melcangi RC, Caruso D, Mitro N: Diabetes-induced myelin abnormalities are associated with an altered lipid pattern: Protective effects of LXR activation. *J Lipid Res* 53:300-310, 2012
- Chung YC, Lim JH, Oh HM, Kim HW, Kim MY, Kim EN, Kim Y, Chang YS, Kim HW, Park CW: Calcimimetic restores diabetic peripheral neuropathy by ameliorating apoptosis and improving autophagy. *Cell Death Dis* 9:1163, 2018
- Currie CJ, Poole CD, Evans M, Peters JR, Morgan CL: Mortality and other important diabetes-related outcomes with insulin vs other antihyperglycemic therapies in type 2 diabetes. *J Clin Endocrinol Metab* 98:668-677, 2013
- Declèves AE, Mathew AV, Armando AM, Han X, Dennis EA, Quehenberger O, Sharma K: AMP-activated protein kinase activation ameliorates eicosanoid dysregulation in high-fat-induced kidney disease in mice. *J Lipid Res* 60:937-952, 2019
- Dirig DM, Salami A, Rathbun ML, Ozaki GT, Yaksh TL: Characterization of variables defining hindpaw withdrawal latency evoked by radiant thermal stimuli. *J Neurosci Methods* 76:183-191, 1997
- Ebato C, Uchida T, Arakawa M, Komatsu M, Ueno T, Komiya K, Azuma K, Hirose T, Tanaka K, Kominami E, Kawamori R, Fujitani Y, Watada H: Autophagy is important in islet homeostasis and compensatory increase of beta cell mass in response to high-fat diet. *Cell Metab* 8:325-332, 2008
- Eid AA, Ford BM, Bhandary B, de Cassia Cavaglieri R, Block K, Barnes JL, Gorin Y, Choudhury GG, Abboud HE: Mammalian target of rapamycin regulates Nox4-mediated podocyte depletion in diabetic renal injury. *Diabetes* 62:2935-2947, 2013
- Eid AA, Ford BM, Block K, Kasinath BS, Gorin Y, Ghosh-Choudhury G, Barnes JL, Abboud HE: AMP-activated protein kinase (AMPK) negatively regulates Nox4-dependent activation of p53 and epithelial cell apoptosis in diabetes. *J Biol Chem* 285:37503-37512, 2010
- Eid AA, Gorin Y, Fagg BM, Maalouf R, Barnes JL, Block K, Abboud HE: Mechanisms of podocyte injury in diabetes: role of cytochrome P450 and NADPH oxidases. *Diabetes* 58:1201-1211, 2009
- Eid S, Abdul-Massih C, El-Khuri C, Hamdy A, Rashid A, Eid A: New mechanistic insights in the development of diabetic nephropathy: Role of cytochromes P450 and their metabolites. *J Endocr Disord* 1:1-6, 2014
- Eid SA, El Massry M, Hichor M, Haddad M, Grenier J, Dia B, Barakat R, Boutary S, Chanal J, Aractingi S, Wiesel P, Szyndralewicz C, Azar ST, Boitard C, Zaatar G, Eid AA, Mas-saad C: Targeting the NADPH oxidase-4 and liver X receptor pathway preserves schwann cell integrity in diabetic mice. *Diabetes* 69:448-464, 2020
- Feldman EL, Nave KA, Jensen TS, Bennett DLH: New horizons in diabetic neuropathy: Mechanisms, bioenergetics, and pain. *Neuron* 93:1296-1313, 2017
- Fernandez AM, Dupont J, Farrar RP, Lee S, Stannard B, Le Roith D: Muscle-specific inactivation of the IGF-I receptor induces compensatory hyperplasia in skeletal muscle. *J Clin Invest* 109:347-355, 2002
- Fortun J, Verrier JD, Go JC, Madorsky I, Dunn WA, Notterpek L: The formation of peripheral myelin protein 22 aggregates is hindered by the enhancement of autophagy and expression of cytoplasmic chaperones. *Neurobiol Dis* 25:252-265, 2007
- Gilani A, Pandey V, Garcia V, Agostinucci K, Singh SP, Schragenheim J, Bellner L, Falck JR, Paudyal MP, Capdevila JH, Abraham NG, Laniado Schwartzman M: High-fat diet-induced obesity and insulin resistance in CYP4a14(-/-) mice is mediated by 20-HETE. *Am J Physiol Regul Integr Comp Physiol* 315:R934-R944, 2018
- Gomez-Sanchez JA, Carty L, Iruarrizaga-Lejarreta M, Palomo-Irigoyen M, Varela-Rey M, Griffith M, Hantke J, Macias-Camara N, Azkargorta M, Aurrekoetxea I, De Juan VG, Jefferies HB, Aspichueta P, Elortza F, Aransay AM, Martinez-Chantar ML, Baas F, Mato JM, Mirsky R, Woodhoo A, Jessen KR: Schwann cell autophagy, myelinophagy, initiates myelin clearance from injured nerves. *J Cell Biol* 210:153-168, 2015
- Gonzalez-Fernandez E, Staursky D, Lucas K, Nguyen BV, Li M, Liu Y, Washington C, Coolen LM, Fan F, Roman RJ: 20-HETE enzymes and receptors in the neurovascular unit: Implications in cerebrovascular disease. *Front Neurol* 11:983, 2020
- Gonzalez CD, Lee MS, Marchetti P, Pietropaolo M, Towns R, Vaccaro MI, Watada H, Wiley JW: The emerging role of autophagy in the pathophysiology of diabetes mellitus. *Autophagy* 7:2-11, 2011
- Hamilton RT, Bhattacharya A, Walsh ME, Shi Y, Wei R, Zhang Y, Rodriguez KA, Buffenstein R, Chaudhuri AR, Van Remmen H: Elevated protein carbonylation, and misfolding in sciatic nerve from db/db and Sod1(-/-) mice: plausible link between oxidative stress and demyelination. *PLoS One* 8: e65725, 2013
- Hasse B, Bosse F, Hanenberg H, Muller HW: Peripheral myelin protein 22 kDa and protein zero: Domain specific trans-interactions. *Mol Cell Neurosci* 27:370-378, 2004
- Hiyama H, Yano Y, So K, Imai S, Nagayasu K, Shirakawa H, Nakagawa T, Kaneko S: TRPA1 sensitization during diabetic vascular impairment contributes to cold

hypersensitivity in a mouse model of painful diabetic peripheral neuropathy. *Mol Pain* 14:1744806918789812, 2018

26. Hotta N, Kawamori R, Atsumi Y, Baba M, Kishikawa H, Nakamura J, Oikawa S, Yamada N, Yasuda H, Shigetani Y, Group AS: Stratified analyses for selecting appropriate target patients with diabetic peripheral neuropathy for long-term treatment with an aldose reductase inhibitor, epalrestat. *Diabet Med* 25:818-825, 2008
27. Huang HC, Chen L, Zhang HX, Li SF, Liu P, Zhao TY, Li CX: Autophagy promotes peripheral nerve regeneration and motor recovery following sciatic nerve crush injury in rats. *J Mol Neurosci* 58:416-423, 2016
28. Li M, Nishimura H, Kusano KF, Qin G, Yoon YS, Wecker A, Asahara T, Losordo DW: Neuronal nitric oxide synthase mediates statin-induced restoration of vasa nervorum and reversal of diabetic neuropathy. *Circulation* 112:93-102, 2005
29. Kellogg AP, Cheng HT, Pop-Busui R: Cyclooxygenase-2 pathway as a potential therapeutic target in diabetic peripheral neuropathy. *Curr Drug Targets* 9:68-76, 2008
30. Kim J, Kundu M, Viollet B, Guan K-L: AMPK and mTOR regulate autophagy through direct phosphorylation of Ulk1. *Nat Cell Biol* 13:132-141, 2011
31. Kisfalvi K, Moro A, Sinnott-Smith J, Eibl G, Rozengurt E: Metformin inhibits the growth of human pancreatic cancer xenografts. *Pancreas* 42:781-785, 2013
32. Lai G, Wu J, Liu X, Zhao Y: 20-HETE induces hyperglycemia through the cAMP/PKA-PhK-GP pathway. *Mol Endocrinol* 26:1907-1916, 2012
33. Lin CH, Cheng YC, Nicol CJ, Lin KH, Yen CH, Chiang MC: Activation of AMPK is neuroprotective in the oxidative stress by advanced glycosylation end products in human neural stem cells. *Exp Cell Res* 359:367-373, 2017
34. Luong TN, Carlisle HJ, Southwell A, Patterson PH: Assessment of motor balance and coordination in mice using the balance beam. *J Vis Exp*, 2011
35. Ma J, Yu H, Liu J, Chen Y, Wang Q, Xiang L: Metformin attenuates hyperalgesia and allodynia in rats with painful diabetic neuropathy induced by streptozotocin. *Eur J Pharmacol* 764:599-606, 2015
36. Maalouf RM, Eid AA, Gorin YC, Block K, Escobar GP, Bailey S, Abboud HE: Nox4-derived reactive oxygen species mediate cardiomyocyte injury in early type 1 diabetes. *Am J Physiol Cell Physiol* 302:C597-C604, 2012
37. Melemedjian OK, Asiedu MN, Tillu DV, Sanoja R, Yan J, Lark A, Khoutorsky A, Johnson J, Peebles KA, Lepow T, Sonenberg N, Dussor G, Price TJ: Targeting adenosine monophosphate-activated protein kinase (AMPK) in pre-clinical models reveals a potential mechanism for the treatment of neuropathic pain. *Mol Pain* 7:70, 2011
38. Menzies FM, Fleming A, Caricasole A, Bento CF, Andrews SP, Ashkenazi A, Fullgrabe J, Jackson A, Jimenez Sanchez M, Karabiyik C, Licitra F, Lopez Ramirez A, Pavel M, Puri C, Renna M, Ricketts T, Schlotawa L, Vicinanza M, Won H, Zhu Y, Skidmore J, Rubinsztein DC: Autophagy and neurodegeneration: pathogenic mechanisms and therapeutic opportunities. *Neuron* 93:1015-1034, 2017
39. Mroueh FM, Noureldein M, Zeidan YH, Boutary S, Irani SAM, Eid S, Haddad M, Barakat R, Harb F, Constantine J, Kanj R, Sauleau EA, Ouhtit A, Azar ST, Eid AH, Eid AA: Unmasking the interplay between mTOR and Nox4: novel insights into the mechanism connecting diabetes and cancer. *FASEB J* 33:14051-14066, 2019
40. Obrosova IG, Stavniichuk R, Drel VR, Shevalye H, Vareniuk I, Nadler JL, Schmidt RE: Different roles of 12/15-lipoxygenase in diabetic large and small fiber peripheral and autonomic neuropathies. *Am J Pathol* 177:1436-1447, 2010
41. Pop-Busui R, Boulton AJ, Feldman EL, Bril V, Freeman R, Malik RA, Sosenko JM, Ziegler D: Diabetic neuropathy: A position statement by the American Diabetes Association. *Diabetes Care* 40:136-154, 2017
42. Rami A, Langhagen A, Steiger S: Focal cerebral ischemia induces upregulation of Beclin 1 and autophagy-like cell death. *Neurobiol Dis* 29:132-141, 2008
43. Rangaraju S, Notterpek L: Autophagy aids membrane expansion by neuropathic Schwann cells. *Autophagy* 7:238-239, 2011
44. Rena G, Hardie DG, Pearson ER: The mechanisms of action of metformin. *Diabetologia* 60:1577-1585, 2017
45. Roy Chowdhury SK, Smith DR, Saleh A, Schapansky J, Marquez A, Gomes S, Akude E, Morrow D, Calcutt NA, Ferryhough P: Impaired adenosine monophosphate-activated protein kinase signaling in dorsal root ganglia neurons is linked to mitochondrial dysfunction and peripheral neuropathy in diabetes. *Brain* 135:1751-1766, 2012
46. Rumora AE, Lentz SI, Hinder LM, Jackson SW, Valesano A, Levinson GE, Feldman EL: Dyslipidemia impairs mitochondrial trafficking and function in sensory neurons. *FASEB J* 32:195-207, 2018
47. Toth P, Csiszar A, Sosnowska D, Tucsek Z, Cseplo P, Springo Z, Tarantini S, Sonntag WE, Ungvari Z, Koller A: Treatment with the cytochrome P450 omega-hydroxylase inhibitor HET0016 attenuates cerebrovascular inflammation, oxidative stress and improves vasomotor function in spontaneously hypertensive rats. *Br J Pharmacol* 168:1878-1888, 2013
48. Vincent AM, Perrone L, Sullivan KA, Backus C, Sastry AM, Lastoskie C, Feldman EL: Receptor for advanced glycation end products activation injures primary sensory neurons via oxidative stress. *Endocrinology* 148:548-558, 2007
49. Wang S, Kobayashi K, Kogure Y, Yamanaka H, Yamamoto S, Yagi H, Noguchi K, Dai Y: Negative regulation of TRPA1 by AMPK in primary sensory neurons as a potential mechanism of painful diabetic neuropathy. *Diabetes* 67:98-109, 2018
50. Wang X, Sun D, Hu Y, Xu X, Jiang W, Shang H, Cui D: The roles of oxidative stress and Beclin-1 in the autophagosome clearance impairment triggered by cardiac arrest. *Free Radic Biol Med* 136:87-95, 2019
51. Wang Z, Yadav AS, Leskova W, Harris NR: Inhibition of 20-HETE attenuates diabetes-induced decreases in retinal hemodynamics. *Exp Eye Res* 93:108-113, 2011
52. Ward NC, Chen K, Li C, Croft KD, Keane JF Jr.: Chronic activation of AMP-activated protein kinase prevents 20-

hydroxyeicosatetraenoic acid-induced endothelial dysfunction. *Clin Exp Pharmacol Physiol* 38:328-333, 2011

53. Webb JL, Ravikumar B, Atkins J, Skepper JN, Rubinsztein DC: Alpha-Synuclein is degraded by both autophagy and the proteasome. *J Biol Chem* 278:25009-25013, 2003

54. Wen H, Ostman J, Bubb KJ, Panayiotou C, Priestley JV, Baker MD, Ahluwalia A: 20-Hydroxyeicosatetraenoic acid (20-HETE) is a novel activator of transient receptor potential vanilloid 1 (TRPV1) channel. *J Biol Chem* 287:13868-13876, 2012

55. Yao F, Zhang M, Chen L: 5'-Monophosphate-activated protein kinase (AMPK) improves autophagic activity in diabetes and diabetic complications. *Acta Pharm Sin B* 6:20-25, 2016

56. Yerra VG, Gundu C, Bachawal P, Kumar A: Autophagy: The missing link in diabetic neuropathy? *Med Hypotheses* 86:120-128, 2016

57. Yerra VG, Kalvala AK, Kumar A: Isoliquiritigenin reduces oxidative damage and alleviates mitochondrial impairment by SIRT1 activation in experimental diabetic neuropathy. *J Nutr Biochem* 47:41-52, 2017

58. Zeng Q, Han Y, Bao Y, Li W, Li X, Shen X, Wang X, Yao F, O'Rourke ST, Sun C: 20-HETE increases NADPH oxidase-derived ROS production and stimulates the L-type Ca²⁺ channel via a PKC-dependent mechanism in cardiomyocytes. *Am J Physiol Heart Circ Physiol* 299:H1109-H1117, 2010

59. Zhang X, El Demerdash N, Falck JR, Munnuri S, Koehler RC, Yang ZJ: The contribution of TRPV1 channel to 20-HETE-Aggravated ischemic neuronal injury. *Prostaglandins Other Lipid Mediat* 137:63-68, 2018

60. Zhang Y, Li J, Wang T, Wang J: Amplitude of sensory nerve action potential in early stage diabetic peripheral neuropathy: An analysis of 500 cases. *Neural Regen Res* 9:1389-1394, 2014